X-ray Diffraction Study of Molten Te and Tl-Te Alloys

Y. Waseda and S. Tamaki *

The Research Institute of Mineral Dressing and Metallurgy, Tohoku University,
Sendai 980, Japan

(Z. Naturforsch. **30 a**, 1655—1660 [1975] ; received July 10, 1975)

X-ray diffraction patterns have been obtained from molten Te at 470, 520 and 570 °C. The heights of the peak maxima in the structure factor were much the same in contrast with those of typical molten metals such as sodium.

Molten Tl-Te alloys have been studied by X-ray diffraction for the alloy compositions 25, 33.3, 50, 60 and 75 at% Te at 500 °C and at about 20 °C above the liquidus. The total structure factors for the 25 and 33.3 at% Te alloys were almost the same as that of pure Tl. This implies that the atomic arrangement of these molten alloys is very close to that of pure Tl. Although a drastic change is not found in the general form of the structure factor, the parameter of the range of local atomic order abruptly increases on passing from Tl_2Te to more Te-rich alloys. The three partial structures were also evaluated from the observed X-ray intensities assuming that each partial structure is independent of the relative abundance of the constituent elements in the alloys.

1. Introduction

Recently, various properties of liquid semiconductors have been discussed [1, 2]. These results suggested that the structure of liquid semiconductors is different from that of typical molten metals such as sodium. But comparatively little work of the structural information has been reported on these liquid semiconductors.

The main purpose of this paper is to determine the atomic distribution of molten Tl-Te alloys by X-ray diffraction, because this alloy system is one of the familiar liquid semiconductors, whose electronic transport properties in the liquid state show a drastic change at Tl_2Te composition.

2. Experimental Procedures

The experimental arrangement and operating procedures for the X-ray intensity measurements on high temperature melts were almost identical with those described in our previous works [3, 4]. The purity of the metal samples used in this work is 99.99% Tl and 99.999% Te, respectively.

3. Analysis of Intensity Patterns

The method of analyzing the measured X-ray intensity was also the same as that described previously [5]. For convenience of discussion, the essential features are given below. Assuming the disordered materials, amorphous solids and liquids, to have a continuous distribution of atoms, the intensity of the coherent X-ray scattering per atom $I_{\text{eu}}^{\text{coh}}(Q)$ which is directly obtained experimentally from more than one species of atoms, can be written as

$$I_{\text{eu}}^{\text{coh}}(Q) = \langle f^2 \rangle + \langle f \rangle^2 \int_0^\infty 4\pi r^2 [\varrho(r) - \varrho_0] \frac{\sin(Qr)}{Qr} \mathrm{d}r\,, \tag{1}$$

where $\langle f^2 \rangle = \sum_i c_i f_i^2$, $\langle f \rangle = \sum_i c_i f_i$; c_i and f_i are the concentration and atomic scattering factor of the atomic species i, $\varrho(r)$ is the radial density function and ϱ_0 is the average number density of atoms. The so-called total structure factor $S(Q)$ for multi-component systems is defined in the form

$$S(Q) = [I_{\text{eu}}^{\text{coh}}(Q) - (\langle f^2 \rangle - \langle f \rangle^2)] / \langle f \rangle^2\,. \tag{2}$$

In the case of one component systems, the structure factor is reduced to the following simple form,

$$S(Q) = I_{\text{eu}}^{\text{coh}}(Q) / f^2\,. \tag{3}$$

From these equations, the atomic radial distribution function $4\pi r^2 \varrho(r)$ is evaluated by the Fourier transform of the structure factor:

$$4\pi r^2 \varrho(r) = 4\pi r^2 \varrho_0 + \frac{2r}{\pi} \int_0^\infty Q[S(Q) - 1] \sin(Qr)\,\mathrm{d}Q\,. \tag{4}$$

The pair distribution function $g(r) = \varrho(r)/\varrho_0$ is also frequently used to discuss the structure of amorphous solids and liquids.

---

* Permanent address: Department of Physics, Faculty of Science, Niigata University, *Niigata 950-21*, Japan.

Reprint requests to Dr. Y. Waseda, The Research Institute of Mineral Dressing and Metallurgy, Tohoku University, *Sendai 980*, Japan.

4. Structure of Molten Te

Figure 1 shows the structure factor $S(Q)$ for molten Te at 470, 520 and 570 °C calculated from measured X-ray intensities together with those by other authors [6–9]. Although the measuring temperatures were slightly different, there is adequate agreement as shown in Figure 1. The pair distribution function $g(r)$ calculated from Eq. (4) with the density measured by Lucas and Urbain [10] and the curves obtained by other authors [6–9] are shown in Figure 2. Tourand and Breuil [6] reported that there are three resolved peaks at 2.96, 3.80 and 4.49 Å at 675 °C in the pair distribution function. This is also found in the results of Hoyer, Thomas and Wobst [9] and of this work. Only Harker, Howe and Enderby [8] did not report the existence of a peak near the distance of 3.80 Å. As shown in Fig. 1, the general form of the structure factor for molten Te is different from that of typical molten metals such as Na. For comparison the structure factor of molten Na at 105 °C [11] is also plotted in Figure 1. The heights of the peak maxima in the structure factor for molten Te are much the same in contrast to those of molten Na. These peak maxima are relatively temperature insensitive within the observed temperature range. The oscillation in the structure factor for molten metals such as Na is damped more rapidly in the high Q region than that of molten Te. This implies that considerable atomic arrangement related to covalent-like bonding remains in the liquid state, because if species with definite bond lengths and angles exist, the oscillation in the structure factor should persist in the high Q region [12]. This behaviour was also found in the case of molten Se[4], although there are differences in detail.

The peak positions and coordination number of atoms evaluated from the atomic radial distribution function $4\pi r^2 \varrho(r)$ are listed in Table 1 together with those of other authors. It is assumed for the derivation of the coordination number of the respective neighbours that the shape of the peak maximum is Gaussian [13]. The interatomic distances for the trigonal structure of Te in the solid state are summarized in Table 2 (see p. 1658).

The first three neighbour distances in molten Te observed in this work correspond to those of the crystalline trigonal structure. But the following points should be noted: The first nearest neighbour distance is larger by 4.1% than the covalent bond distance of 2.835 Å and the coordination number of this correlation area is approximately three as shown in Table 1. In contrast to this the coordination number of nearest neighbour atoms for solid and liquid Se is two [4] and the second and third neighbour distances shift inward. This is one of the differences in the structures of molten Te and Se. X-ray diffraction experiments in this work show that the atomic arrangement of Te changes on melting. This is consistent with the physical properties such as the electrical conductivity [1, 2]. Therefore it seems that, contrary to molten Se[4], the atomic arrangement of molten Te is not composed of minute trigonal crystals.

The atomic arrangement of trigonal type structures is not as close packed as that of typical metallic elements. As the melting of Te is accompanied by a

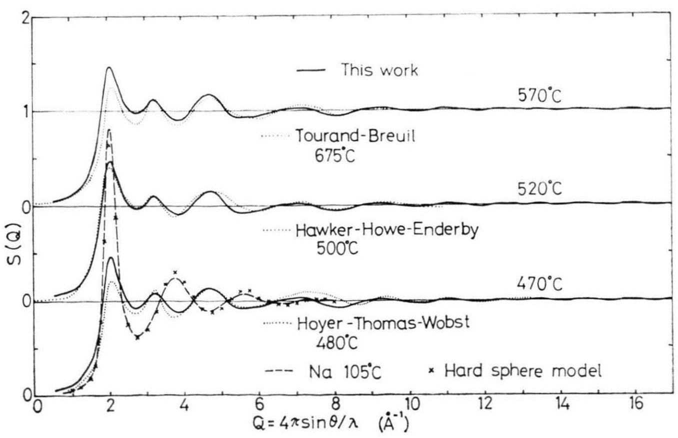

Fig. 1. Structure factor of molten Te at 470, 520 and 570 °C.

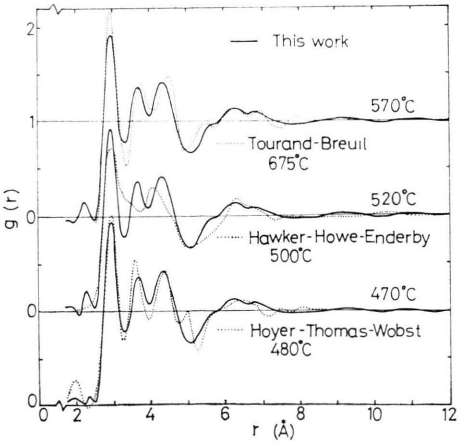

Fig. 2. Pair distribution function of molten Te at 470, 520 and 570 °C.

Table 1. Summary of diffraction results from liquid tellurium.

	radiation	temp. [°C]	structure factor [Å^{-1}] 1st max	1st min	2nd max	2nd min	pair distribution function [Å] r_1	r_2	r_3	coordination number (atoms) n_1	n_2	n_3	n
Tourand		675	2.1	2.65	3.2	3.7	2.96	3.80	4.49	3.18	3.25	7.06	13.5
Breuil	Neutron	900	—	—	—	—	3.01	3.82	4.52	3.36	3.12	6.84	13.3
(1971)*		1100	—	—	—	—	3.01	3.80	4.52	3.72	2.81	7.15	13.7
Howker Howe Enderby (1973)	Neutron	500 800	(2.1)**	(2.8)	(3.2)	(3.8)	(2.95)	(4.2)	(6.4)	—	—	—	—
Hoyer		480	2.10	2.70	3.35	3.75	2.95	3.55	4.45	2.98	2.85	6.35	12.2
Thomas	X-ray	550	2.15	2.70	3.25	3.75	2.95	3.55	4.25	2.98	2.79	6.36	12.1
Wobst (1975)		620	2.15	2.70	3.25	3.75	2.95	3.55	4.25	3.01	2.82	6.48	12.3
This		470	2.10	2.75	3.20	3.85	2.95	3.67	4.32	3.03	2.85	6.43	12.3
work	X-ray	520	2.10	2.80	3.20	3.90	2.95	3.65	4.28	3.12	2.83	6.47	12.4
		570	2.10	2.80	3.20	3.90	2.96	3.67	4.28	3.14	2.79	6.45	12.4

* This work was carried out at temperatures between 575 and 1700 °C But both structure factor and distribution function were reported at 675, 900 and 1100 °C. $n = n_1 + n_2 + n_3$.

** The parentheses denote the estimated values from the original figures by the present authors. The values previously reported in the work of Enderby and Hawker (J. Non-cryst. Solids **8—10**, 687 [1972]) are not necessarily in agreement with those of figures.

density change of about 5%, the local atomic arrangement evidently changes to an antimony-like arrangement on melting. This is plausible because the electronic properties of molten Te rather show a metallic character [1] corresponding to the large electrical resistivity of molten Sb, which is more than three times that of typical molten metals. In the antimony-like arrangement of atoms, each atom has three nearest neighbours (n_1) at the distance r_1 with three other (n_2) slightly farther away near the distance of $r_2 = 1.16\, r_1$. The third nearest neighbours are six atoms (n_3) near the distance of $r_3 = 1.48\, r_1$. According to these arrangements, r_1, r_2 and r_3 are 2.95 Å, 3.42 Å and 4.37 Å, respectively. As shown in Table 1, the experimental results obtained in this work support this interpretation. It is also supported by the fact that the average number of atoms (n) in the short range order, defined as $n = n_1 + n_2 + n_3$, observed exprimentally and listed in the last column of Table 1 is nearly equal to the value 12 of the antimony-like arrangement of atoms. On the other hand, the value of n is 14 in the case of a trigonal type structure. These facts are also found in the work of Hoyer, Thomas and Wobst [9].

5. Structure of Molten Tl-Te Alloys

For convenience of the discussion a few additional details on the analysis of intensity patterns are given below. It is well-known that the structure of multi-component disordered systems is characterized by the partial distribution functions $\varrho_{ij}(r)$. In general, $\varrho_{ij}(r)$ means the number of j-type atoms per unit volume at the distance r from an i-type atom. The partial distribution function $\varrho_{ij}(r)$ is connected with the partial structure factor $S_{ij}(Q)$ by the equation [14, 15]

$$S_{ij}(Q) = 1 + \int_0^\infty 4\,\pi\, r^2 \left[\frac{\varrho_{ij}(r)}{c_j} - \varrho_0\right] \frac{\sin(Q\,r)}{Q\,r}\,\mathrm{d}r\,. \tag{5}$$

The partial pair distribution function $g_{ij}(r) = \varrho_{ij}(r)/(c_j\,\varrho_0)$ is frequently used. The total structure factor $S(Q)$ directly obtained by experiments is then the weighted sum of the partial structure factors $S_{ij}(Q)$. In the case of a binary alloy, we can write

$$S(Q) = \sum_i \sum_j w_{ij}\, S_{ij}(Q) = w_{ii}\, S_{ii}(Q) + w_{jj}\, S_{jj}(Q) + 2\, w_{ij}\, S_{ij}(Q)\,, \tag{6}$$

where w_{ij} is the weighting factor defined by

$$w_{ij} = c_i\, c_j\, f_i\, f_j / \langle f \rangle^2\,. \tag{7}$$

A) Total Structure Factors

The total structure factors of molten Tl-Te alloys, measured isothermally at 500 °C, are shown in

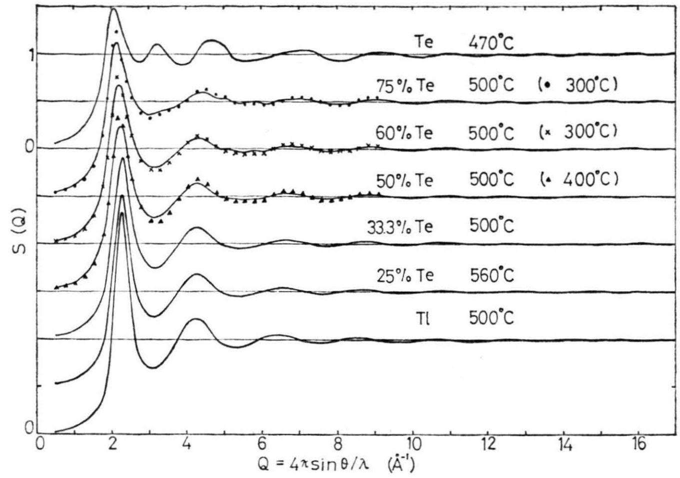

Table 2. Interatomic distances for trigonal structure of Te in the solid stale.

interatomic distance [Å]	coordination number (atoms)
2.835	2
3.50	4
4.44 4.46	8
4.89	4
5.28	4
5.93	2
6.02	2

Fig. 3. Total structure factors of molten Tl-Te alloys.

Figure 3. The measurements were performed at 560 °C in the case of the 25 at % Te alloy. The measurements were also carried out at temperatures about 20 °C above the liquidus for the 50, 60 and 75 at % Te alloys and the results obtained are also plotted in Figure 3. The effect of temperature on the total structure factors of molten Tl-Te alloys consists in the fact, that the height of the peak maxima is reduced and that they are broadened. These tendencies are generally found in most molten alloy systems. The discussion in this work is limited to the data measured isothermally at 500 °C. The error bars in these measurements are of the order of ± 0.09 over the first peak, ± 0.04 near the value of $Q = 4.0$ Å^{-1} and ± 0.02 beyond $Q = 6.0$ Å^{-1}.

The total structure factors of molten the 25 and 33.3 at-% Te alloys are almost the same as that of pure Tl and the first peak position decreases gradually from 2.26 Å^{-1} for the 33.3 at-% Te alloy to 2.10 Å^{-1} for pure Te. The general form of the total structure factor for molten Tl-Te alloys is relatively insensitive to the Te concentration as shown in Figure 3. This is caused by the larger scattering power of the Tl atoms in the weighting factors w_{ij} of Equation (6). The total structure factor $S(Q)$ for molten alloys beyond the Te concentration of Tl_2Te toward the Te rich side is asymmetric, in that the low angle side of the first peak maximum is less steep than the high angle side. This behaviour was also confirmed by measurements with Cu radiation. In this analysis, the separation of the scattered intensity from the primary beam in the small angle region ($Q \leqq 2.0$ Å^{-1}), the correction for air scattering and absorption and the elimination of the Laue monotonic scattering ($\langle f^2 \rangle - \langle f \rangle^2$) to evaluate the total structure factor $S(Q)$ by means of Equation (2) were carefully taken account of. The asymmetry of the first peak, mentioned earlier, must be related to the covalent-like character of molten Te.

The information on the atomic arrangement in real space given by Eq. (4) seems to be suitable for the discussion of the structure in molten alloys. Figure 4 shows the total pair distribution function for the molten Tl-Te alloys. All the curves of $g(r)$ oscillate around unity. Although an apparent change is not observed in the total structure factor, the effect of Te concentration on the structure is easily

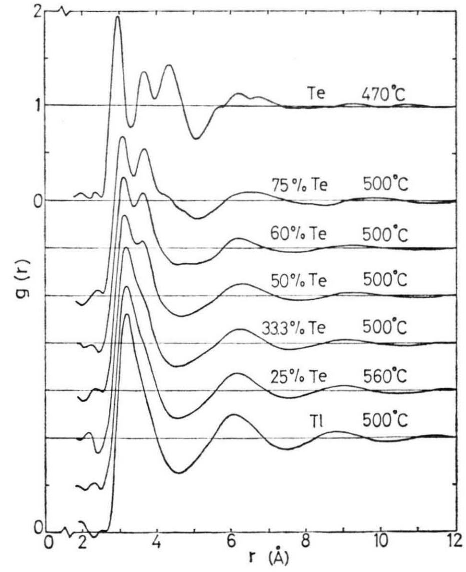

Fig. 4. Total pair distribution functions of molten Tl-Te alloys.

found in the total pair distribution function. A subsidiary peak on the larger distance side of the first peak is observed in the case of the 33.3 at-% Te alloy. But the general form of $g(r)$ for this alloy is similar to that of pure Tl as well as the 25 at-% Te alloy. Beyond the Te concentration 50 at-%, a new peak appears near 3.65 Å. This position corresponds to that of the second nearest neighbour in pure Te. The decay of the amplitude in the oscillation and the distortion of the wave pattern are also found with increasing Te concentration.

The coordination number of atoms is one of the useful parameters to discuss the structure of disordered systems. But, as shown in Fig. 4, the Gaussian curves to estimate the coordination number of the respective neighbours are not easily drawn in the case of the 33.3, 50 and 60 at-% Te alloys. For this reason, the structure of molten Tl-Te alloys is discussed in the following way in this work. The pair distribution function $g(r)$ can be used to estimate the range of local atomic order. In this work we introduce the assumption that this range is limited by a radius r_s beyond which $g(r)=1\pm0.02$. The value of ±0.02 is considered to be a reasonable choice for the errors in $g(r)$ at larger r. This approach was also used in the work on metallic glasses [16]. The value of r_s estimated for the molten Tl-Te alloys are listed in Table 3. We also introduce a dimensionless parameter $\zeta=r_s/r_1$ as the measure of the range of local atomic order, where r_1 is the nearest neighbour distance. As shown in Fig. 5, the parameter ζ changes abruptly near the composition of Tl_2Te from about 4.0 to about 4.4 times.

Table 3. Values of peak positions in the pair distribution function and the parameter of local order atomic arrangement.

	r_1 (Å)	r_2' (Å)	r_2'' (Å)	r_2 (Å)	r_s (Å)
Tl−O at% Te	3.24	—	—	6.15	13.0
25	3.22	—	—	6.24	13.0
33.3	3.20	sub.	—	6.26	13.0
50	3.14	3.62	—	6.25	13.5
60	3.08	3.65	—	6.24	13.5
75	3.06	3.66	—	6.35	13.4
100	2.95	3.67	4.32	6.25	12.8
Tl-Tl	3.20	—	—	6.10	13.0
Tl-Te	3.13	3.70	5.02	6.40	13.0
Te-Te	2.96	3.65	4.34	6.30	12.5

The results on the total structure factor, the total pair distribution function and the parameter of the local atomic order imply that the atomic arrangement of the Tl rich alloys is very close to that in pure Tl, whereas that of alloys containing more Te than Tl_2Te is similar to that in pure Te. This may suggest that the matrix arrangement of atoms in molten Tl-Te alloys changes from the arrangement as observed in Tl melts to that observed in Te melts near the composition of Tl_2Te. This statement is consistent with the fact that the electronic transport properties of these alloys in the liquid state show a drastic change at Tl_2Te composition [1, 2].

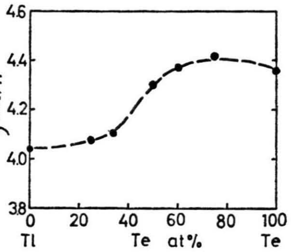

Fig. 5. Concentration dependence of the parameter of the range of local atomic order ζ for molten Tl-Te alloys.

B) Partial Structure Factors

As easily found in Eq. (6), $S_{\text{Tl-Tl}}(Q)$, $S_{\text{Te-Te}}(Q)$ and $S_{\text{Tl-Te}}(Q)$ can be calculated from the total structure factors $S(Q)$ of the alloys, assuming that each partial structure factor is independent of the relative abundance of the constituent elements in the alloys. This approach was already discussed in detail and frequently gave some information on the structure of a binary alloy.

The calculation was performed to derive the partial structure factors from the data on the 50, 60 and 75 at-% Te alloys and then the best fit values of $S_{\text{Tl-Tl}}(Q)$, $S_{\text{Te-Te}}(Q)$ and $S_{\text{Tl-Te}}(Q)$ were determined by a least square analysis of five total structure factors with different Te concentrations. Figures 6 and 7 show the partial structure factors $S_{ij}(Q)$ and the partial pair distribution functions $g_{ij}(r)$, respectively. The peak positions in Fig. 7 and the parameters of local atomic arrangement calculated from Fig. 7 are summarized in the lower part of Table 3. The method of evaluating these quantities is the same as above. As shown in Figs. 6 and 7, the partial structures of like atom pairs (Tl-Tl and Te-Te) are close to those of the pure elements. This seems to indicate that the partial structures are independent of the compostion of the molten Tl-Te alloys. However, it should be kept in mind that the partial structures estimated in this work are rather applicable for the Te rich alloys beyond the Te

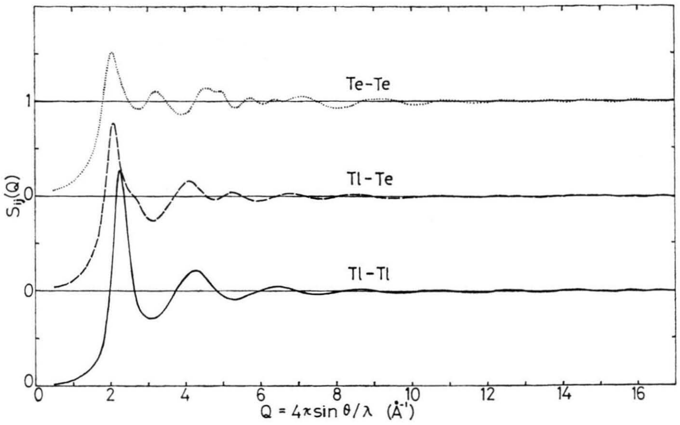

Fig. 6. Partial structure factors of molten Tl-Te alloys.

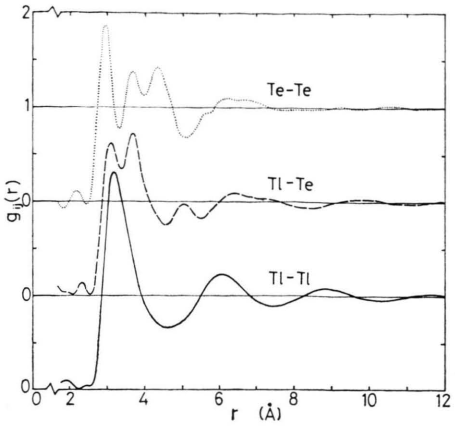

Fig. 7. Partial pair distribution functions of molten Tl-Te alloys.

concentration of Tl_2Te, which show the same order of r_1 and ζ (see Table 3). Although the covalent-like character of pure Te partially disappears as Tl is added to molten Tl-Te alloys, the partial structures estimated are consistent with a more or less random mixture of Tl and Te atoms. If strong compound formation or ordering (i.e. Tl_2Te molecules) as evidenced by a premaximum below the first peak maximum in $S(Q)$ or $S_{ij}(Q)$ occurs in a binary alloy system, the partial structures cannot be assumed to be independent of composition. Such behaviour has been observed in molten Mg-based [17, 18] and Li-based alloys [19]. However, it is apparent that the structure of molten Tl-Te alloys does not indicate any premaxima and is represented by the combination of three partial structures of atom pairs (Tl-Tl, Te-Te and Tl-Te).

Acknowledgements

Most of this work was carried out at The Research Institute of Mineral Dressing and Metallurgy, Tohoku University. The authors are greatly indebted to Prof. M. Ohtani for his support and encouragement in this study. We would also like to thank the members of the Computer Centre, Tohoku University for allowing the use of their computer.

[1] M. H. Cohen and G. Lucovsky (Editors), Proceeding of International Conference on the Properties of Amorphous and Liquid Semiconductors, Michigan Conference, J. Non-Cryst. Solids **8—10**, 676 [1972].

[2] J. Tauc (Editor), Amorphous and Liquid Semiconductors, Plenum Press, London 1974.

[3] Y. Waseda and M. Ohtani, Phys. Stat. Sol. (b) **62**, 535 [1974].

[4] Y. Waseda, K. Yokoyama, and K. Suzuki, Phys. Cond. Matter **18**, 293 [1974].

[5] Y. Waseda and T. Masumoto, Z. Phys. B **21**, 235 [1975].

[6] G. Tourand and M. Breuil, J. de Physique **32**, 813 [1971].

[7] J. E. Enderby and J. Hawker, J. Non-Cryst. Solids **8—10**, 687 [1972].

[8] J. E. Enderby, in Ref. 2, p. 361.

[9] W. Hoyer, E. Thomas, and M. Wobst, Z. Naturforsch. **30 a**, 235 [1975].

[10] L. D. Lucas and G. Urbain, R. Acad. Sci. Paris **255**, 3406 [1962].

[11] Y. Waseda and S. Tamaki, unpublished.

[12] P. A. Egelstaff, D. I. Page, and J. G. Powles, Mol. Phys. **20**, 881 [1971].

[13] Y. Waseda, K. Suzuki, S. Tamaki, and S. Takeuchi, Phys. Stat. Sol. **39**, 181 [1970].

[14] C. N. J. Wagner, Liquid Metals, Chemistry and Physics, S. Z. Beer (Editor), Marcel Dekker, New York 1972.

[15] D. T. Keating, J. Appl. Phys. **34**, 923 [1963].

[16] C. N. J. Wagner, J. Vac. Sci. Technol. **6**, 650 [1969].

[17] W. E. Lukans and C. N. J. Wagner, Z. Naturforsch. **28 a**, 297 [1973].

[18] S. Steeb and R. Hezel, Z. Metallk. **57**, 374 [1966].

[19] K. Goebbels and H. Ruppersberg, Proceeding of International Conference on the Properties of Liquid Metals, Tokyo Conference, S. Takeuchi (Editor), Taylor and Francis, London 1973, p. 63.